Monitoring spike differentiation stages of winter wheat based on land surface temperature time series and Kalman Filter

Liu Junming[1,2*], Pan Peizhu[1,2], Wang Pengxin[1,2], Cui Zhenzhen[1,2], Hu Xin[3]

(1. *College of Information and Electrical Engineering, China Agricultural University, 100083 Beijing, China*;
2. *Key Laboratory of Remote Sensing for Agri-Hazards, Ministry of Agriculture, 100083 Beijing, China*;
3. *Wheat Research Institute, Shangqiu Academy of Agriculture and Forestry Sciences, 476000 Shangqiu, China*)

Abstract: Spike differentiation is an important reproductive growth process of winter wheat, and monitoring spike differentiation stages is also a significant part of phenology monitoring of winter wheat. By taking Shangqiu, Henan Province as the study area, the paper aims to study the methodology of monitoring spike differentiation stages of winter wheat at regional scale based on assimilation remote sensing LST data with crop growth model. Firstly, the paper established the equation between air temperature at the height of 1.5 m above wheat field and LST after green-turning stage of winter wheat. On this basis, the air temperature was used as assimilated quantity, and Kalman Filter algorithm was applied to assimilate air temperature converted from MODIS LST time series data with air temperature time series data which obtained by Inverse Distance Weighted (IDW) to get the consequent air temperature time series data of wheat field in the whole period of winter wheat. Then, WheatGrow model which can simulate the growth and development of wheat was introduced and calibrated to obtain spike differentiation stages of winter wheat based on the assimilated air temperature time series data. The results showed that: (1) The trend of assimilated air temperature was consistent with the trend of interpolated air temperature, but its spatial variation was close to that of LST. The assimilation effect of daily minimum air temperature was significantly better than daily maximum air temperature, the determination coefficient R^2 of minimum air temperature was 0.94 but only 0.70 for maximum air temperature between assimilation and observation. (2) The study can realize the monitoring of floret differentiation stage, stamen and pistil differentiation stage, anther separation stage, tetrad differentiation stage at regional scale. The validated results showed that the deviation of start date between simulation and observation of spike differentiation stages was less than 5 days, and the deviation of duration was in range of 1 to 4 days.

Keywords: spike differentiation stages, data assimilation, Kalman Filter, WheatGrow model, winter wheat

Citation: Liu, J. M., P. Z. Pan, P. X. Wang, Z. Z. Cui, and X. Hu. 2017. Monitoring spike differentiation stages of winter wheat based on land surface temperature time series and Kalman Filter. International Agricultural Engineering Journal, 26(3): 385–398.

1 Introduction

Spike differentiation is an important reproductive growth process of winter wheat (González et al., 2003; Serrago et al., 2008; Mcmaster et al., 1992), and monitoring spike differentiation stages is also a significant part of phenology monitoring of winter wheat. The traditional method for identifying spike differentiation stages of wheat is mainly estimated by the corresponding relationship between the development of wheat spike and the leaf formation of plant or the elongation of plant stem (Cui et al., 2006; Steinmeyer et al., 2013; Jamieson et al., 2007). However, as the spike differentiation process of wheat is affected by climate conditions, wheat variety characteristics, and cultivation measures, etc, the internal reproductive growth of wheat plant is not completely consistent with the vegetative growth of external organ, so the accuracy of identifying spike differentiation stages of wheat by using such method is relatively low. It is possible to accurately identify the spike differentiation stages by using the method of anatomical observation in the laboratory after field sampling. However, this method is not suitable for

Received date: 2017-06-28 **Accepted date:** 2017-08-19
***Corresponding author: Liu Junming**, Ph.D., Associate Professor of College of Information and Electrical Engineering, China Agricultural University, Beijing 100083,China. Tel: 13910693390, Email: liujunming2000@163.com.

continuous observation of regional spike differentiation process of wheat and it is also destructive to the crop itself.

Along with the in-depth study of basic theory of plant physiology and ecology, CERES-Wheat (Abrecht et al., 1996; Jones et al., 2003; Dettori et al., 2011), APSIM-Wheat (Keating et al., 2003; Balwinder-Singh et al., 2011) and WheatGrow (Cao et al., 1997; Yan et al., 2000; Yan et al., 2000; Zun-Fu et al., 2013) and other wheat growth models based on photosynthesis, respiration, transpiration, nutrition and other mechanism process of wheat have gradually developed, which can accurately simulate the growth and development process of wheat. Among them, WheatGrow model, a growth model based on the mechanism of spike differentiation of wheat established by Cao et, al, can quantitatively provide the identification index of spike differentiation stages, and realize the simulation of winter wheat spike differentiation stages on single point scale and in denomination of "Day". However, as the simulation of spike differentiation stages is developed from single-point studies to regional application, the increase of spatial scale may lead to many difficulties in the acquisition of some macro data and the parameter regionalization (Jin et al., 2012).

Satellite remote sensing technology has the advantages of acquiring surface information extensively, real-timely and periodically. It has a good complementary relationship with the advantages of the crop model featured with strong mechanism and continuous process orientation and time. By coupling the crop model and remote sensing information, the temporal and spatial continuity of crop monitoring can be realized, thus greatly improving the simulation accuracy of crop model. Land surface data assimilation is an effective means to realize the coupling between crop model and remote sensing information (Dorigo et al., 2007; Liu et al., 2013; Xie et al., 2016). The correction of key input parameters in crop model by taking real-time remote sensing information as observational variable and through the adoption of data assimilation method can effectively improve the simulation accuracy of crop model, and enable the single point simulation of crop growth model to develop into regional application (Ren et al., 2011; Li et al., 2015; Xie et al., 2015).

Long-time and continuous air temperature time series data is one of the most important input parameters to drive the operation of WheatGrow model. How to obtain accurate spatio-temporal continuous air temperature time series data sets is the key to extend the WheatGrow model from single point to regional application, and realize the monitoring of spike differentiation stages of winter wheat within a region. At present, the air temperature data is mainly obtained from designated points at long-term observation meteorological stations distributing within the study area. The temperature time series data sets at regional scale is difficult to obtain due to the restrictions on economic and technical conditions, and limited number and uneven distribution of long-term observation meteorological stations within the study area. Although air temperature values at unknown points at regional scale can be estimated by use of the method of spatial interpolation, yet the interpolation results are very uncertain due to the influence of topography, density and distribution of sample points and interpolation method, etc (Noi et al., 2016; Liu et al., 2013; Xu et al., 2011). In addition, in terms of the crop, its growth and yield formation are directly affected by the field microclimate where it exists (Liu et al., 2015), and meteorological stations are usually located at the edge of city or suburban open space. Influenced by urban heat island effect and underlying surface, there are differences between the air temperature of meteorological station and interpolation and farmland. For this reason, the characteristics of air temperature of farmland can't be truly reflected.

In this paper, by basing upon the WheatGrow model, taking winter wheat as the object of study, and regarding air temperature as the assimilated quantity, the author adopts the Kalman Filter Algorithm to assimilated air temperature data time series interpolated and land surface temperature (LST) of remote sensing to obtain the air temperature time series data above the wheat field, and then realizes the monitoring of spike differentiation stages of winter wheat at regional scale.

2 Study area and data

2.1 Study area

Located in the east of Henan Province and the hinterland of Huang-Huai Plain, Shangqiu is one of the main producing area and high yield area within Huang-Huai wheat area (Liu et al., 2016). Located between east longitude 114°49′-116°39′ and northern latitude 33°43′-34°52′, this area belongs to semi-moist continental monsoon climate within the warm temperate zone with annual mean air temperature reaching around 14°C, mean annual sunshine duration 2205-2427 h, annual mean precipitation 623 mm, and annual average frost-free period 211 d. Semi-winterness variety is dominant in the winter wheat plantation. The perennial sowing time of winter wheat is generally during the first 10 days to the second 10 days of October, and the green-turning stage is during the third 10 days of February. The jointing stage is during the second to third 10 days of March, the heading stage is during the second to third 10 days of April, and the maturation stage is during the end of May until the start of June. The study area is as shown in Figure 1.

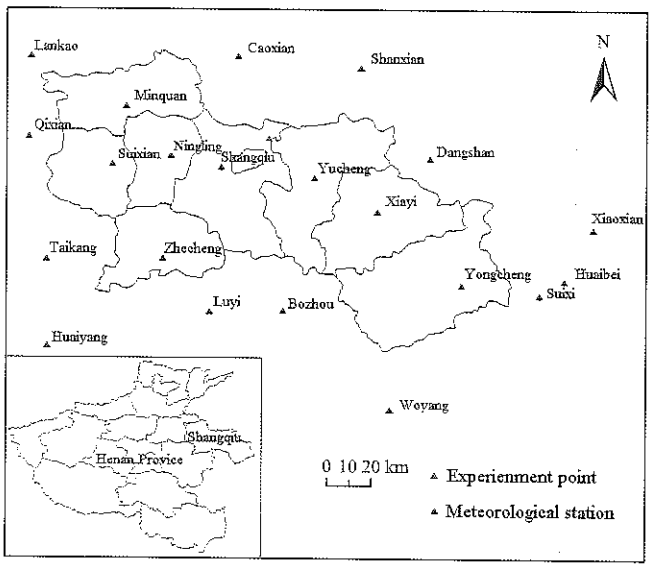

Figure 1 Map of the study area

2.2 Data

2.2.1 Meteorological data

The meteorological data mainly include the time series of daily maximum air temperature and minimum air temperature at a total of 21 meteorological stations (Figure 1) spreading within and around the municipal district of Shangqiu, Henan Province during the winter wheat growth period from 2015 to 2016. Next, the meteorological data also comprise the daily maximum air temperature, minimum air temperature and phenological data of winter wheat at Shangqiu base station (34°27′N, 115°40′E, elevation: 50.1 m) during the winter wheat growth period from 2005-2006 and 2014-2015. Such data is used for the calibration of WheatGrow model. The above data are derived from China Meteorological Data Network (http://data.cma.cn/).

In addition,2016 agro-meteorological weekly report information published by Shangqiu Meteorological Bureau (http://www.sqqxj.gov.cn/ggqx/nyqxzb/) is also consulted in this study, so as to acquire the green-turning stage, jointing stage, booting stage, heading stage and other critical phenological periods of winter wheat in Shangqiu.

2.2.2 Remote sensing data

The remote sensing data includes: ① Daily surface temperature product of MYD11A1 acquired by MODIS Aqua satellite during the winter wheat growth period in Shangqiu from 2015 to 2016. The spatial resolution is 1km. ② MCD12Q1, three-level land cover product of MODIS with spatial resolution of 500 m. As the study on spike differentiation stages of winter wheat is meaningful only in the winter wheat growing area, it is thus required to extract the winter wheat growing area according to the Land Cover Type5 scheme in MCD12Q1. Remote sensing data are derived from LAADS Web (http://ladsweb.nascom.nasa.gov /data /search.html), and raw data need to be pre-processed by means of embedding, projection, clipping, and etc.

2.2.3 Measured data

Measured data are mainly used to validate the results of spike differentiation stages of winter wheat. The field experiment of spike differentiation stages was conducted at Shuangba testing field of the Test and Demonstration Center under Henan Shangqiu Academy of Agriculture and Forestry Sciences (34°31′55″N, 115°42′37″E, elevation: 50.1 m), the locally common semi-winterness variety of Wenmai 6 was taken as the testing variety, the sowing date was determined at October 15th and the heading stage was generally entered at around April 18th of the next year.

During March 12th to May 31st, 2016, real-time observation and records were conducted with respect to the growth of Wenmai 6 in the experimental field. The procedures mainly comprised ① Air temperature observation of upper underlying surface: Air temperature sensors were arranged at the height of 1.5 m above the wheat field, for the real-time measurement of air temperature above the wheat field. The effective range of sensor measurement is –20°C-60°C, accuracy ±0.5°C, and frequency once per hour. ② Observation of biological indicators: 5-10 wheat plants having uniform and representative growth vigor were taken from the experiment field after washing off mud, so as to determine and record the plant height, tiller number, leaf age of main stem and internodal length of each wheat seedling at every 2-3d. ③ Definition of spike differentiation stages: The main stem of wheat seeding was taken as the object of observation, dissected and placed under the binocular microscope, so as to observe the spike differentiation process and take photos for recording purpose. The descriptions and illustrations for division of spike differentiation stages (compiled by Cui et al., 2006) were taken as the specific reference data for observation of spike differentiation stages, so as to observe and record the specific dates (mainly including the beginning and ending dates of floret differentiation stage, stamen and pistil differentiation stage, anther separation stage, tetrad differentiation stage) emerging from all stages of spike differentiation stages after the green-turning stage of winter wheat. Meanwhile, the beginning date of heading stage in the experiment field was also observed and recorded.

3 Method

3.1 WheatGrow model

In this research, WheatGrow model, i.e. the process-based mechanism wheat growth and development, was taken as a dynamic model which can quantitatively describe the spike differentiation process at the top of wheat stem via PDT (Physiological Development Times). Spike differentiation stages enter into the next stage when PDT has accumulated to a specified value. The PDT threshold values corresponding to floret differentiation stage, stamen and pistil differentiation stage, anther separation stage, tetrad differentiation stage and heading stage are 14.5, 16.1, 17.9, 21.4 and 26.8, respectively (Yan et al., 2000).

In order to simulate the spike differentiation stages of winter wheat, the WheatGrow model needs to be localized and calibrated, and the calibration process is mainly aimed to determine TS (Temperature Sensitivity), PS (Photoperiod Sensitivity), PVT (Physiological Vernalization Time) and IE (Intrinsic Earliness)variety parameters required by the model operation. However, these parameters are difficult to be directly observed. Wenmai 6, a locally common variety of winter wheat, was taken as the standard crop, and the loop iteration for optimization method was adopted to solve the parameter values of calibrated varieties. Specific methods can be described as follows, (1) the average sowing date of winter wheat was determined at October 15th, the average emergence of seedlings date October 21st, the heading date April 17th, and the average duration from emergence of seedlings to heading 178 d according to the phonological observation data of winter wheat during 2005-2006 and 2014-2015 at Shangqiu base station. (2) In the light of the literature (Yan et al., 2000), it is determined that the value ranges for TS, PVT, PS and IE of Wenmai 6 were [1.4, 1.5], [20, 25], [0.004, 0.005] and [0.80, 0.85], respectively. The cycle step sizes for four parameters were separately configured as 0.01, 1, 0.0001 and 0.01. (3) Based on the above parameters, the daily maximum air temperature, minimum air temperature data during the period of 2005-2006 to 2014-2015 at Shangqiu base station, as well as the seeding date, value range of variety parameters and step sizes as determined in No. (1) step, it was possible to run the WheatGrow model on loop iteration basis, calculate the average number of days after extracting the number of days for emergence of seedling until heading obtained from each time of operation, compare the number of days with the standard number of days, and determine the variety parameters combination with minimum difference value as the optimum variety parameter combination. The value ranges for ultimately-determined TS, PS, PVT and IE were 1.5, 0.0048, 25 and 0.85, respectively.

3.2 Spatial interpolation of air temperature

In this paper, in order to obtain the meteorological data of Shangqiu within the growth period of winter wheat, IDW (Inverse Distance Weighted) (Bayazit et al., 2016; Ozelkan et al., 2015) was adopted on account of daily maximum and minimum air temperature data at meteorological stations within and around the municipal district of Shangqiu, so as to generate, via interpretation, the daily maximum and minimum air temperature time series data within the growth period of winter wheat during 2015-2016. The specific calculation formula is described as follows:

$$\lambda_i = \frac{1}{d_i^2} / \sum_{i=1}^{n} (\frac{1}{d_i^2}) \quad (1)$$

$$Z = \sum_{i=1}^{n} \lambda_i Z_i \quad (2)$$

where, λ_i stands for the weight; n stands for the number of meteorological stations for interpretation purpose; d_i stands for the measured distance between interpolating point and No. i meteorological stations. Z stands for the estimated air temperature value of interpolation. Z_i stands for the measured air temperature value corresponding to No. i (i=1,2,3.....n) meteorological stations.

3.3 Establishment of LST and air temperature linear regression model above wheat field

Analysis of the correlation between MODIS LST and the measured air temperature above the wheat field is the key to applying the remote sensing data in the monitoring of winter wheat spike differentiation stages at regional scale. Through the interaction between Terra satellite and Aqua satellite of MODIS, the LST (Land Surface Temperature) data in the same region can be obtained on daily basis. The transit time of Terra satellite is around 10:30 and 22:30, respectively. The transit time of Aqua satellite is around 13:30 and 01:30, respectively. In consideration of the fact that the maxiumum air temperature usually takes place in the afternoon, while the occurrence time of minimum air temperature is relatively close to the transit time at around 01:30, the linear regression was conducted in this paper by respectively extracting LST products (i.e. MYD11A1_Day and MYD11A1_Night) of Aqua satellite within the observed period of field and the daily maximum and minimum air temperature at the height of 1.5m above the wheat field (Figure 2). The regression equations are listed as follows:

$$[AIRT_{\max}] = [LST\_day] * 1.1805 - 3.6711 \quad (3)$$

$$[AIRT_{\min}] = [LST\_night] * 0.8931 + 0.9232 \quad (4)$$

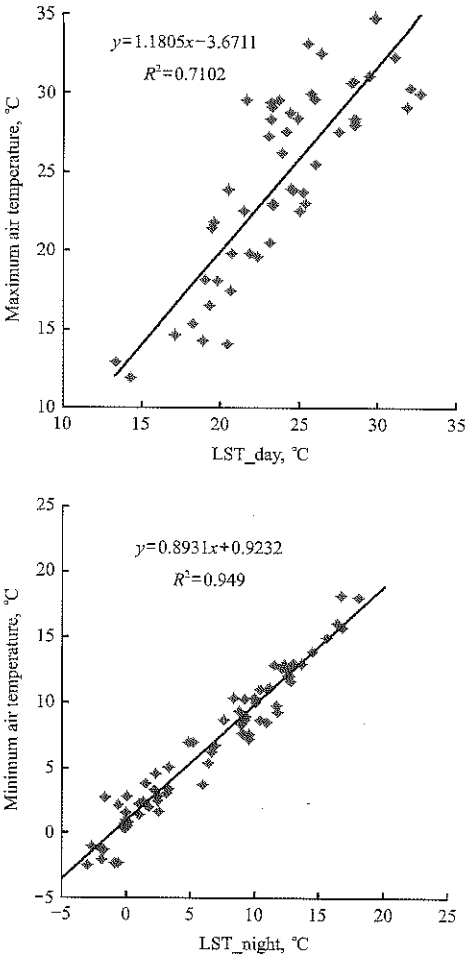

Figure 2 Regression analysis of LST and air temperature of 1.5 m height in wheatfield

3.4 Kalman Filter assimilation algorithm

As a recursive prediction algorithm based on statistical theory, KF (Kalman Filter) algorithm obtains the optimal estimated value of required physical parameters by processing the observational data containing noise and through the adoption of linear unbiased minimum variance estimation method (Peng, 2009; Anadranistakis et al., 2002; Libonati et al., 2008). By combining the model simulation values with the external observation values in the estimation of target parameters, it can effectively reduce the error of estimation process and improve the prediction accuracy. In this study, the continuous air temperature time series above the wheat field was generated at regional scale by

taking land surface temperature products of MODIS as the source of external observation data and by assimilating the air temperature data obtained by interpolation sequentially through the adoption of KF algorithm. The specific recurrence formulas are as follows:

$$Y_t^f = X_t B_{t-1} \tag{5}$$

$$R_t = C_{t-1} + W \tag{6}$$

$$\sigma_t = X_t R_t X_t^T + V \tag{7}$$

$$A_t = R_t X_t^T \sigma_t^{-1} \tag{8}$$

$$B_t = B_{t-1} + A_t (Y_t^o - Y_t^f) \tag{9}$$

$$C_t = R_t - A_t \sigma_t A_t^T \tag{10}$$

where, Y_t^f stands for the estimated value of air temperature, X_t stands for daily maximum and minimum air temperature data at meteorological stations within and around the municipal district of Shangqiu during the winter wheat growth period. B_{t-1} stands for the coefficient vector of interpolation, i.e. weight value λ in the inverse distance weighted of air temperature; R_t stands for the error covariance matrix of extrapolated value B_t, C_{t-1} is the error covariance matrix of B_{t-1}. W stands for the dynamic noise error covariance matrix, σ_t stands for the forecast error covariance matrix; X_t^T stands for the transposed matrix of X_t. V stands for the error covariance matrix of observation noise. A_t stands for the gain matrix, σ_t^{-1} stands for the inverse matrix of σ_t, Y_t^o stands for the "truth-value" of air temperature. That is, the air temperature value at the height of 1.5 m above the wheat field can be obtained from the calculation via formula (3) and (4) by use of MODIS LST product. The recursion of next-step B_t and C_t value can be realized by use of the formula (9) and (10) according to the prediction error.

3.5 Accuracy verification method

MBD (Mean Bias Deviation), MAD (Mean Absolute Deviation) and RMSD (Root Mean Square Deviation) can be selected as indicators for the evaluation of difference between assimilated temperature and measured temperature. Meanwhile, these indicators can also be used as indictors to evaluate the simulation accuracy of spike differentiation stages in WheatGrow model. The specific calculation formulas are as follows:

$$MBD = \frac{1}{N}\sum_1^N (M_i - S_i) \tag{11}$$

$$MAD = \frac{1}{N}\sum_1^N |M_i - S_i| \tag{12}$$

$$RMSD = \sqrt{\frac{1}{N}\sum_1^N (M_i - S_i)^2} \tag{13}$$

where, M_i stands for the simulated value; S_i stands for the measured value; N stands for the number of observation samples. MBD reflects the true deviation, the value of the positive and negative, and the value is closer to zero means the smaller deviation; MAD is used to express the overall prediction accuracy, RMSD is used to express the degree of discretization,and the smaller value of MAD and RMSD the smaller the deviation.

4 Results

4.1 Air temperature assimilation

4.1.1 Air temperature assimilation of single point

Shuangba testing field in Shangqiu was taken as the sample point for the analysis of results of single point air temperature assimilation. The comparison of assimilated air temperature, interpolated and converted air temperature from LST are as shown in Figure 3. It can be found out from Figure 3 that the trend of assimilated air temperature is consistent with the trend of interpolated air temperature, while the values of assimilation are very close to the air temperature converted from LST by linear regression equation. This regular pattern has the same performance at both the maximum and the minimum air temperature. It shows that the air temperature value of assimilation is mainly affected by LST (land surface temperature), the LST level plays the decisive role in the assimilated air temperature, yet the contribution of interpolated air temperature is relatively small. Therefore, subject to the regulation of LST, the maximum air temperature curve of assimilation is above the interpolated maximum air temperature curve, while the minimum air temperature curve of assimilation is below the interpolated minimum air temperature curve.

The deviation between the assimilated air temperature and measured air temperature was further analyzed with MBD, MAD and RMSD. The results are as shown in Figure 4. It can be found out in Figure 4 that R^2 (determination coefficient of assimilated maximum air

temperature and measured maximum air temperature) reached 0.70, the overall deviation was controlled at around 3°C, in which MBD was only 0.8°C. The assimilation effect of the minimum air temperature was better than that of the maximum air temperature, R^2 (determination coefficient of assimilated minimum air temperature and measured minimum air temperature) reached 0.94, MBD, MAD and RMSD were 0.1°C, 1.0°C and 1.3°C, respectively. If compared with maximum air temperature the smaller deviation manifested in the maximum air temperature, the above analysis shows that the air temperature assimilated by KF conforms to the variation characteristics of air temperature of wheat field, and fits for being taken as the input parameter of WheatGrow model for the simulation of spike differentiation stages of winter wheat.

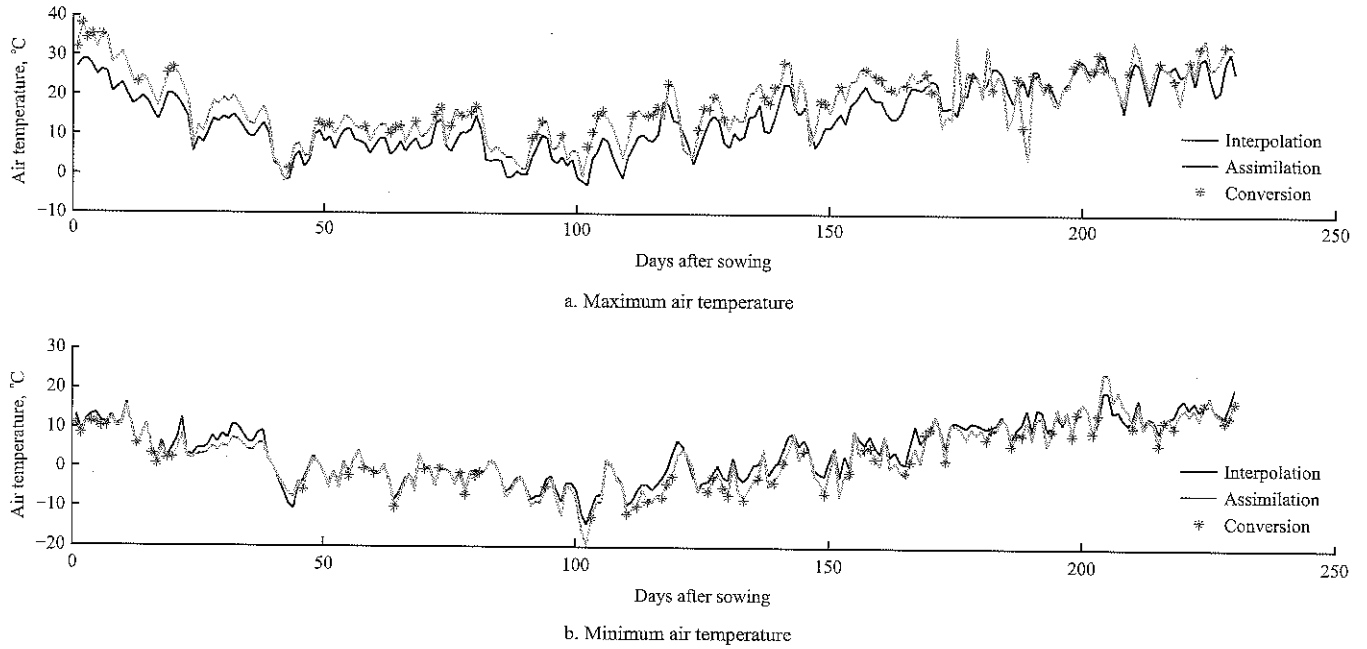

Figure 3 Comparison of assimilated air temperature and interpolated and converted air temperature from LST of 2015-2016

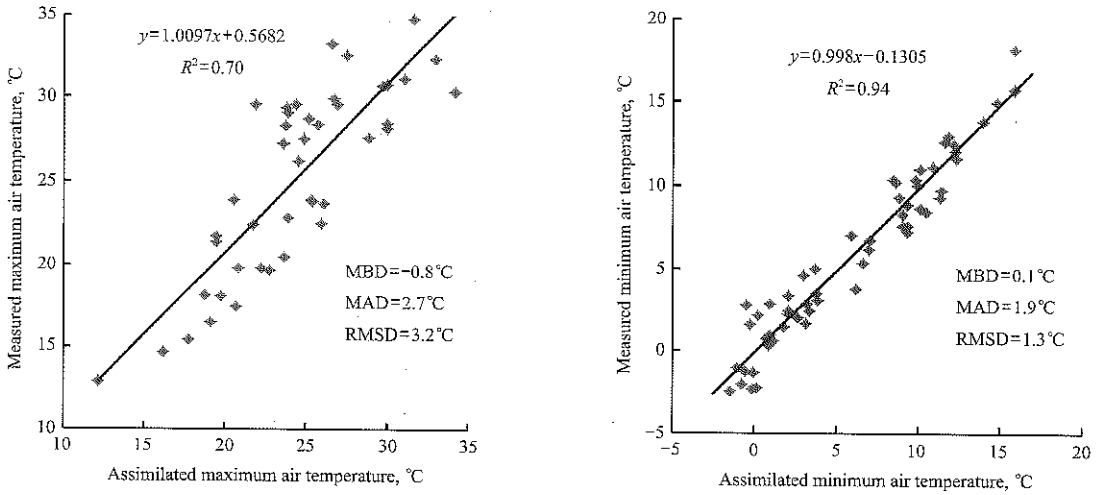

Figure 4 Comparison of air temperature between assimilation and observation

4.1.2 Regional air temperature assimilation

Results of regional air temperature assimilation during the growth period of winter wheat within 2015-2016 were obtained by extending the algorithm to the region scale on the basis of single point air temperature of assimilation. In Figure 5, by taking March 22nd, 2016 as an example, the comparisons between assimilation by KF and MODIS LST products and interpolation by IDW of maximum and minimum air temperatures within the winter wheat planting area of Shangqiu were revealed.

As shown in the figure above, the spatial variability of air temperature of assimilation has kept the variation characteristics of the original MODIS LST remote

sensing images. In the aspect of maximum air temperature, it can be observed from Figure 5a that the maximum air temperature dated March 22nd, 2016 within the north central and northwestern border districts of Shangqiu reached the maximum value of the study area, and the maximum air temperature of assimilation (Figure 5c) also reflected this feature. As shown in the maximum air temperature of interpolation by IDW, the maximum air temperature dated March 22nd, 2016 within the study area ranged between 18°C and 21°C, while the maximum air temperature of assimilation within most areas ranged around 23°C-26°C due to the impact of LST, indicating the obvious effect of LST on assimilated results. Compared with the maximum air temperature, the effect of LST on the assimilated results of minimum air temperature is more obvious. As shown in the comparisons between Figures 5d and 5f, the spatial variation tendency of these two images is almost the same, most of the minimum air temperatures of assimilation are less than 5°C, and the higher minimum air temperature concentrates on the western region. According to the above analysis, it can be observed at the regional scale that the spatial variation of air temperature of assimilation is closer to the variation characteristics of LST, and this regular pattern is more obvious in the assimilated results of minimum air temperature.

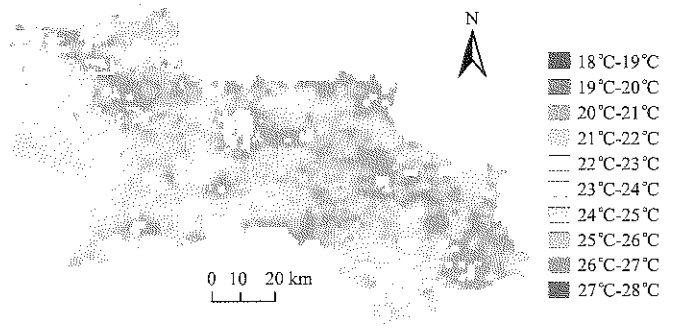

a. MODIS LST_day

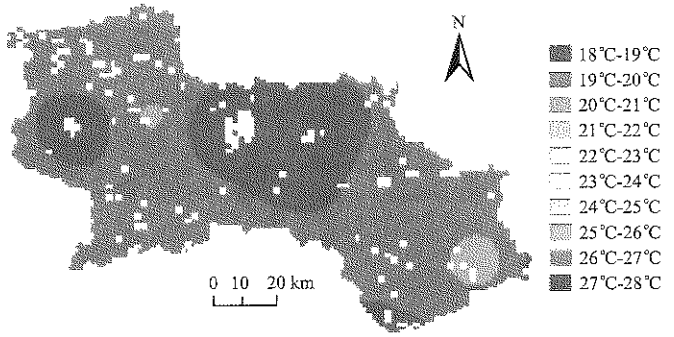

b. Interpolated maximum air temperature by IDW

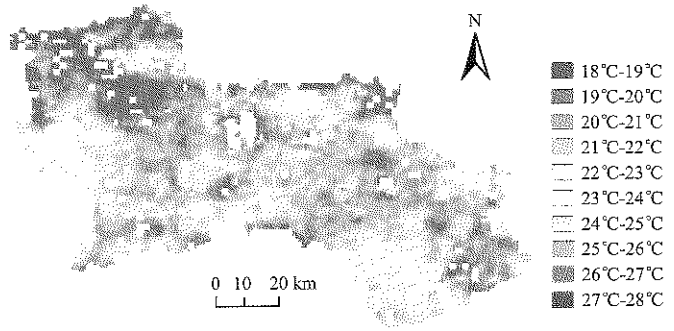

c. Assimilated maximum air temperature by KF

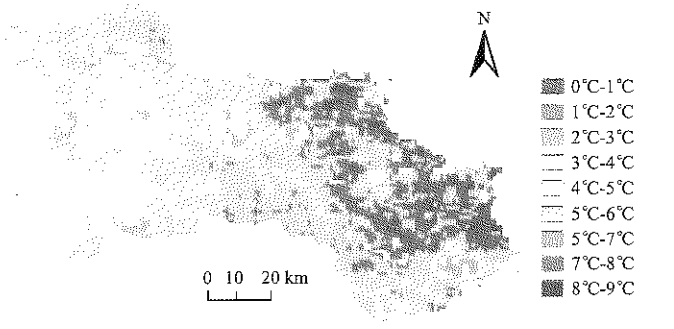

d. MODIS LST_night

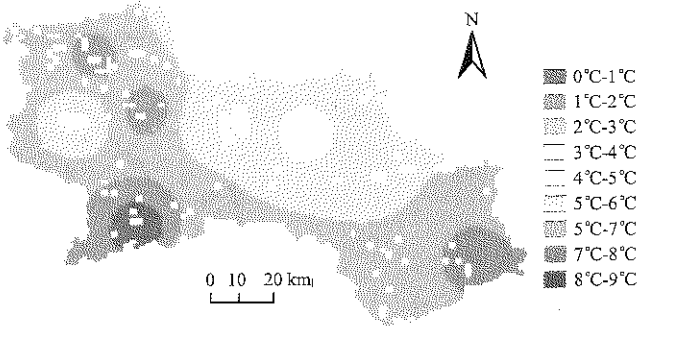

e. Interpolated minimum air temperrature by IDW

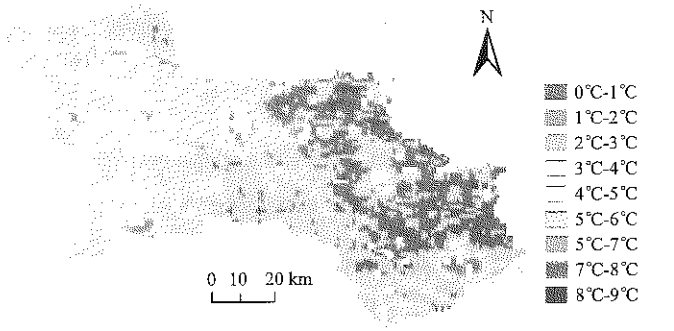

f. Assimilated minimum air temperature by KF

Figure 5 Comparison of assimilated air temperature of winter wheat planting areas in Shangqiu on March 22nd

4.2 Monitoring of spike differentiation stages

4.2.1 Monitoring of regional spike differentiation stages

According to the above analysis, the distribution chart (Figure 6) of the start dates corresponding to the entry of floret differentiation stage, stamen and pistil differentiation stage, anther separation stage, tetrad

differentiation stage and heading stage after the green-turning stage of winter wheat can be obtained at regional scale by inputting the regional maximum and minimum air temperature time series of assimilation during 2015-2016 into WheatGrow model. In this Figure, the start dates corresponding to each of spike differentiation stage were indicated with the number of days after the emergence of seedlings.

As is shown in Figure 6, the overall spatial distribution of the start dates corresponding to all spike differentiation stages (from floret differentiation stage to heading stage) present the trend of gradual delay from south to north. The start dates of spike differentiation stages was the earliest in Zhecheng and Yongcheng county in the south of Shangqiu, while it was the latest in Minquan county in the north of Shangqiu. In addition, the start dates of spike differentiation stages in the north of Yucheng was also relatively late, the maximum time difference was eight days, and such variation became stable in spike differentiation stages from floret differentiation stage to heading stage.

As is shown in Figure 6a, the start dates corresponding to the floret differentiation stage in Shangqiu during 2015-2016 ranged between 143 d and 151 d after the emergence of seedlings, i.e. March 12^{th}-20^{th}. In the majority of districts, the start dates corresponding to the floret differentiation stage concentrated on about 147-149 d after the emergence of seedlings, the start dates of Zhecheng and Yongcheng in the south concentrated on 143-145 d after the emergence of seedlings, the start dates of floret differentiation stage in Minquan (located in the northwest) and Yucheng (located in the northern region) was the latest.

Following the entry of stamen and pistil differentiation stage, the spatial distribution of start dates still presented the trend of gradual transition from south to north, and the start dates was 149-158d after the emergence of seedlings, i.e. March 18^{th}-27^{th}. As indicated in Shangqiu agricultural meteorological weekly data, jointing stage of winter wheat began to spread during March 21^{th}-28^{th}, 2016, and the start dates of stamen and pistil differentiation stage conformed to the statement as mentioned in the literature (Yan et al., 2000) that there is a good synchronization between the stamen and pistil differentiation stage and phenological jointing stage, showing that the monitoring results of spike differentiation stage was consistent with the actual growth status of winter wheat.

As also indicated in Figure 6b, the start dates of stamen and pistil differentiation stage within the planting area of winter wheat in Suixian, Ningling and Xiayi began about 151-153 d after the emergence of seedlings (March 20-22^{nd}), while the start dates of stamen and pistil differentiation stage of the winter wheat planting area within the municipal district of Shangqiu and Yucheng was relatively late, manifesting the spatial distribution differences distinctly different from those of floret differentiation stage at the start dates. According to the agricultural meteorological information weekly, during March 13^{th} to March 19^{th}, 2016. The average air temperature in Yucheng and the municipal district of Shangqiu was obviously low, if compared with that of Suixian and Ningling, etc. Moreover, the extreme minimum temperature of –3.3°C even appeared at Shangqiu base station. Thus, the start dates of stamen and pistil differentiation stage lagged behind.

The spatial distribution of start dates when the spike differentiation stage entered into anther separation stage and tetrad differentiation stage was shown in Figure 6c and 6d, and it can observed that the start dates of anther separation stage began at 155-163 d after the emergence of seedlings (March 24^{th} - April 1^{st}), while the start dates of tetrad differentiation stage began at 163-171 d after the emergence of seedlings (April 1^{st}-9^{th}). It can be observed from the comparison of these two figures that the start dates of anther separation stage and tetrad differentiation stage maintained almost the same spatial distribution, showing that the temperature fluctuation trends and amplitudes of all regions were relatively consistent within the time period when the spike differentiation of winter wheat entered into the stamen and pistil differentiation stage and tetrad differentiation stage during 2015-2016.

With the advance of spike differentiation of winter wheat, the spatial difference of start dates of spike differentiation stage presented the decreasing trend, especially in Minquan in the northwest. Although the

start dates of floret differentiation stage was later than that of other regions, there was no significant differences between the start dates of heading stage of remaining regions.

As is shown in Figure 6e, until about 173 d after the emergence of seedlings, i.e. during the second ten days of April, the winter wheat in Zhecheng started to enter into the heading stage, and successively heading started in remaining regions during 175-178 d after the emergence of seedlings (April 13^{th}-16^{th}), except that the heading dates in the municipal district of Shangqiu and the northern area of Yucheng were relatively late. The result was basically consistent with the ground monitoring results recorded in Shangqiu agricultural meteorological weekly in 2016.

The spike differentiation of winter wheat is a continuous changing process, and the start date of next spike differentiation stage is the end date of previous spike differentiation stage. Thus, the duration of each spike differentiation stages can be calculated. During 2015-2016, the duration of floret differentiation stage in Shangqiu lasted 6-7 d days,the duration of stamen and pistil differentiation stage lasted 5-6 d, anther separation stage and tetrad differentiation stage lasted 8 d and 10 d, respectively. It was roughly consistent with the variation trend of the duration of actual spike differentiation stages.

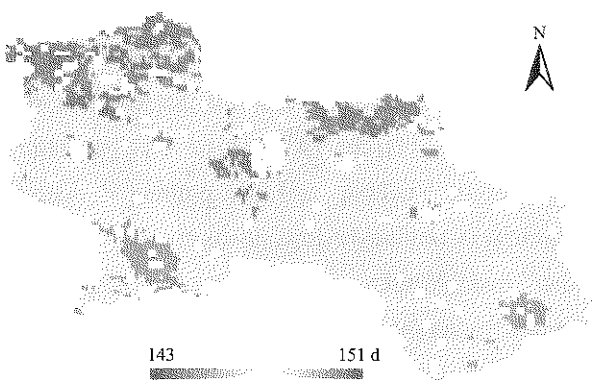

a. Floret differentiation stage

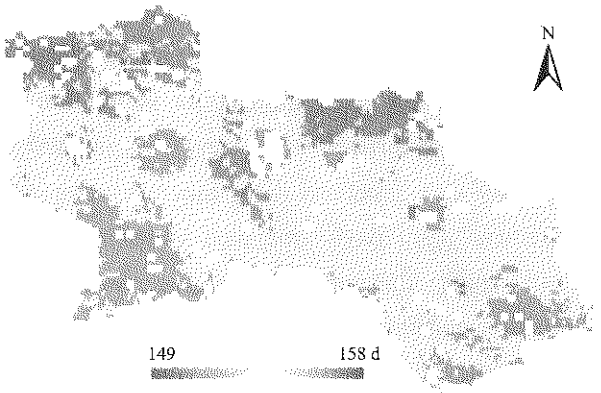

b. Stamen & pistil differentiation stage

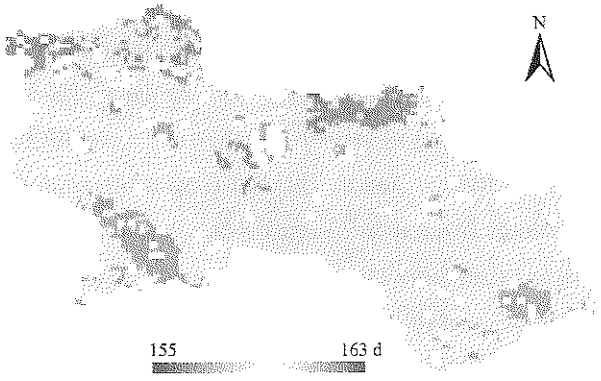

c. Anther separation stage

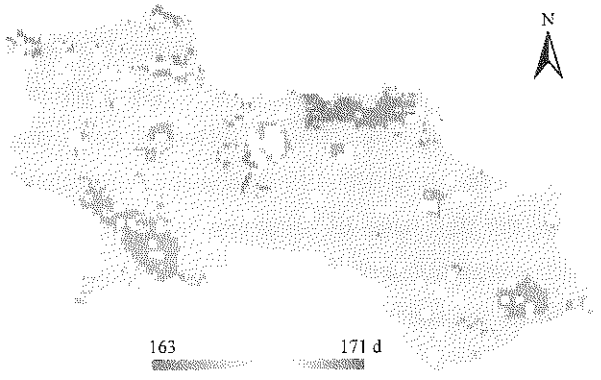

d. Tetrad differentiation stage

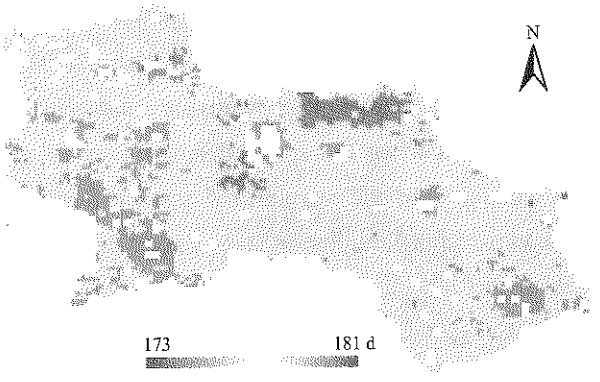

e. Heading stage

Figure 6 Map of the start date of spike differentiation stages in Shangqiu from 2015 to 2016

4.2.2 Verification of spike differentiation stages

According to the above analysis, the start dates of every spike differentiation stage and duration of every stage were obtained through calculation by taking Shuangba Experimental Base as a sample point, and putting the maximum air temperature time series data and minimum air temperature time series data during the winter wheat growth period during 2015-2016 obtained by assimilation, geographic latitude of the experimental field and other parameters into WheatGrow model. Moreover, comparison validation was also conducted by use of the observed results of spike differentiation stages, and the results are shown in Figure 7, Tables 1 and 2.

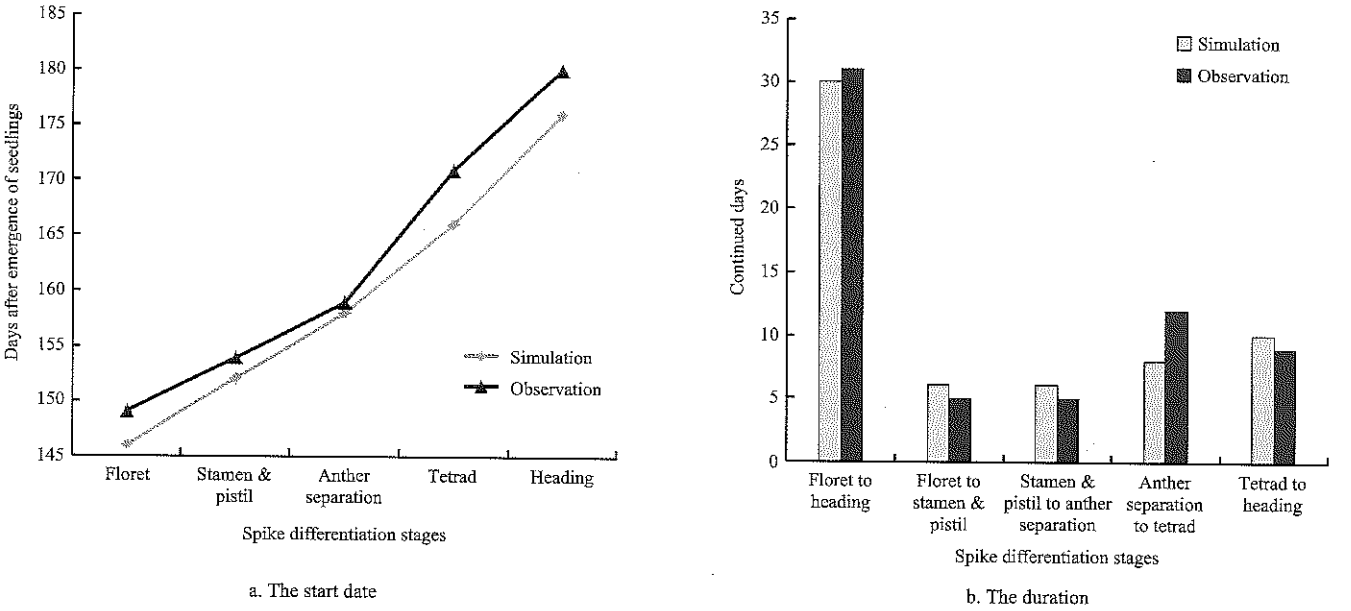

Figure 7 Comparison of start date and duration of spike differentiation stages between simulation and observation from 2015 to 2016

Table 1 Comparison of start date of spike differentiation stages between simulated data and observed data

Category	Floret initiation	Stamen and pistil initiation	Anther separation	Tetrad	Heading	MBD	MAD	RMSD
Simulation	3/15	3/21	3/27	4/4	4/14	-	-	-
Observation	3/18	3/23	3/28	4/9	4/18	-	-	-
ΔD	–3	–2	–1	–5	–4	–3	3	3.3

Note:ΔD represents the deviation between simulated start date and the observed start date of spike differentiation stages.

Table 2 Comparison of duration of spike differentiation stages between simulated data and observed data

Category	Floret to Stamen and pistil	Stamen and pistil to Anther separation	Anther separation to Tetrad	Tetrad to Heading	Floret to Heading	MBD	MAD	RMSD
Simulation	6	6	8	10	30	-	-	-
Observation	5	5	12	9	31	-	-	-
Δd	1	1	–4	1	–1	–0.3	1.8	4.4

Note: Δd represents the deviation of duration of spike differentiation stages between simulated data and observed data, the continued days from Floret to Heading was not used to calculate MBD, MAD and RMSD.

As shown in Figure 7, the overall variation trend of start dates and duration of every spike differentiation stages calculated by WheatGrow model was consistent with the field. As indicated in Table 1 and Table 2, (1) the MBD and MAD between start date of every spike differentiation stage calculated by WheatGrow model and the measured date were all 3 d, RMSD was 3.3 d. Among them, there were relatively large deviations in tetrad differentiation stage (deviation was 5 d). For the rest of every spike differentiation stage, the deviations between simulated date and measured date were less than 5 d, indicating that the validation effect of the start date of every winter wheat spike differentiation stage was good. (2) The deviations of duration between simulation and observation during every spike differentiation stage (calculated by the WheatGrow model) were controlled within 4 d, MBD was 0.3 d, MAD was 1.8 d and RMSD was 4.4 d. Among them, the difference value at the anther

separation-tetrad stage was the largest, i.e. 4 d; The duration of floret-pistil and stamen, stamen and pistil - anther separation, and tetrad-heading was 1 d longer than the measured number of days, while the duration of anther separation-tetrad was shorter than the measured number of days. However, judging from the total number of days of floret-heading, the number of days was very close to the measured number of days under the premise of calculation based on WheatGrow model, i.e. error is only 1 d. It showed that WheatGrow model was ideal for the estimation effect of duration of winter wheat spike differentiation stages.

5 Discussions

In this study, the following several issues still remain to be discussed:

(1) As the air temperature converted by linear regression model with MODIS LST products during assimilation process was taken as "truth-value", thus such value was directly affected by MODIS LST and linear regression equation. For this reason, the precision of assimilation air temperature decreases if MODIS LST extracted is low in accuracy or the effect of linear fitting is poor.

(2) MODIS LST products are the key to realize assimilation by KF. In practice, MODIS LST products may be absent due to cloud pollution. In this paper, the way to deal with this problem can be described as follows, when LST absence appears, it is required to select the LST value when LST was not absent at last moment and take it as the LST at current moment for the continuation of assimilation by KF, which may cause the air temperature of assimilation during the LST-absent time interval to maintain the variation trend of assimilation result at the last moment when LST was not absent. This is obviously out of line with reality, and it is considered to re-conduct assimilation by KF after the reconfiguration of absent LST.

(3) The spike differentiation stages of winter wheat is not only affected by climatic conditions, but also closely related to characteristics of wheat varieties and cultivation measures (Cui et al., 2006; Yang et al., 2007; Steinmeyer et al., 2013; Han et al., 2011). In this paper, only semiwinterness wheat variety was taken as the object of study, for the calibration of WheatGrow model. The parameters calibrated are not entirely suitable for winter and spring wheat varieties.

6 Conclusions

In this paper, under the premise of calibrated WheatGrow model, spatio-temporal continuous air temperature time-series data above the wheat field during the growth period of winter wheat in Shangqiu was obtained by assimilating MODIS LST data and air temperature interpolated by IDW with Kalman Filter. The monitoring of every spike differentiation stage after the green-turning stage of regional winter wheat was realized by the maximum air temperature and minimum air temperature time series of assimilation. The main conclusions are listed as follows:

(1) The continuous air temperature time-series data above the wheat field was obtained by basing upon KF data assimilation algorithm and integrating the advantages of remote sensing technology and crop growth model. The variation trend of assimilated air temperature time-series in wheat field was basically identical to that of the spatial interpolation, yet its spatial variation was closer to that of LST. The determination coefficient R^2 of maximum air temperature was 0.70 and 0.94 for minimum air temperature between assimilation and observation, indicating that the air temperature assimilated by KF complied with the variation characteristics of air temperature in wheat field and fitted as the input parameter of WheatGrow model for the simulation of spike differentiation stages of winter wheat.

(2) Judging from the monitoring results of winter wheat spike differentiation stages, remote sensing technology, geographic information system, spatial interpolation technology and data assimilation technology were integrated in this paper, so as to realize the monitoring of floret differentiation stage, stamen and pistil differentiation stage, anther separation stage, tetrad differentiation stage and heading stage after the green-turning stage of winter wheat. As shown in validated results with single-point, the deviations of start date between simulation and observation during every

spike differentiation stage were within 5 d, and the deviations of duration between simulation and observation during every spike differentiation stage were within 1-4 d. The monitoring result and measured result during the spike differentiation stages were basically identical. The method presented in this paper provides a direction for monitoring spike differentiation stages of winter wheat rapidly, accurately and effectively, and it is of far-reaching significance to the late frost monitoring and yield estimation and relevant researches of winter wheat.

Acknowledgements

This research was supported by the National Natural Science Foundation of China (Grant No.41471342). We thank Shangqiu Academy of Agriculture and Forestry Sciences for the experiment of spike differentiation stages of winter wheat.

[References]

[1] Abrecht, D. G., and S. D. Robinson. 1996. TACT: a tactical decision aid using a CERES based wheat simulation model. *Ecological Modelling*, 86(2-3): 241–244.

[2] Anadranistakis, M., K. Lagouvardos, V. Kotroni, and K. Skouras. 2002. Combination of kalman filter and an empirical method for the correction of near surface temperature forecasts: application over greece. *Geophysical Research Letters*, 29(16): 1776–1779.

[3] Balwinder, S., D. S. Gaydon, E. Humphreys, and P. L. Eberbach. 2011. The effects of mulch and irrigation management on wheat in punjab, india-evaluation of the APSIM model. *Field Crops Research*, 124(1): 1–13.

[4] Bayazit, Y., R. Bakis, and C. Koc. 2016. Mapping distribution of precipitation, temperature and evaporation in seydisuyu basin with the help of distance related estimation methods. *Journal of Geographic Information System*, 08(2): 224–237.

[5] Cao, W., and D. N. 1997. Modelling phasic development in wheat: a conceptual,integration of physiological components. *Journal of Agricultural Science*, 129(2): 163–172.

[6] Cui, J., and T. Guo, 2006. *Spike of Wheat*. Beijing: China Agricultural Press.

[7] Dettori, M., C. Cesaraccio, A. Motroni, D. Spano, and P. Duce. 2011. Using CERES-Wheat to simulate durum wheat production and phenology in Southern Sardinia, Italy . *Field Crops Research*, 120(1): 179–188.

[8] Dorigo, W. A., R. Zurita-Milla, A. J. W. D. Wit, J. Brazile, R. Singh, and M. E. Schaepman. 2007. A review on reflective remote sensing and data assimilation techniques for enhanced agroecosystem modeling. *International Journal of Applied Earth Observation and Geoinformation*, 9(2): 165–193.

[9] González, F. G., G. A. Slafer, and D. J. Miralles. 2003. Floret development and spike growth as affected by photoperiod during stem elongation in wheat. *Field Crops Research*, 81(1): 29–38.

[10] Han, J. L., Q. Yang, W. P. Wang, L. I. Yan-Sheng, and Y. F. Zhou. 2011. Effects of sowing date on the caulis and tillers differentiation of young spike and yield in winter wheat. *Journal of Triticeae Crops*, 32(1): 303–307.

[11] Jamieson, P. D., I. R. Brooking, M. A. Semenov, G. S. Mcmaster, J. W. White, and J. R. Porter. 2007. Reconciling alternative models of phenological development in winter wheat. *Field Crops Research*, 103(1): 36–41.

[12] Jin, H., J. Wang, Y. Bo, G. Chen, and H. Xue. 2012. Estimation on regional maize yield based on assimilation of remote sensing data and crop growth model. *Transactions of the Chinese Society of Agricultural Engineering*, 28(6): 162–173.

[13] Jones, J. W., G. Hoogenboom, C. H. Porter, K. J. Boote, W. D. Batchelor, and L. A. Hunt. 2003. The DSSAT cropping system model. *European Journal of Agronomy*, 18(3-4): 235–265.

[14] Keating, B. A., P. S. Carberry, G. L Hammer, M. E. Probert, M. J. Robertson, and D. Holzworth. 2003. An overview of APSIM, a model designed for farming systems simulation. *European Journal of Agronomy*, 18(3-4): 267–288.

[15] Li, Z., X. Jin, C. Zhao, J. Wang, X. Xu, G. Yang, and J. Shen. 2015. Estimating wheat yield and quality by coupling the DSSAT-CERES model and proximal remote sensing. *European Journal of Agronomy*, 71: 53–62.

[16] Libonati, R., I. Trigo, and C. C. Dacamara. 2008. Correction of 2m-temperature forecasts using kalman filtering technique. *Atmospheric Research*, 87(2): 183–197.

[17] Liu, C., G. Cao, and M. Zhang. 2013. Influence of temporal and uariablity on estimation of air temperatures from MODIS land surface temperatures. *Remote Sensing Technology and Application*, 28(5): 931–835.

[18] Liu, J., M. Li, P. Wang, and J. Huang. 2013. Monitoring of phenology by reconstructing LAI time series data for winter wheat. *Transactions of the Chinese Society of Agricultural Engineering*, 29(19): 120–129.

[19] Liu, J., N. Wang, P. Wang, X. Hu, and J. Huang. 2015. Simulation of air temperature within winter wheat near-ground layer based on SHAW model. *Transactions of the Chinese Society for Agricultural Machinery*, 46(Supp.): 274–282.

[20] Liu, J., N. Wang, P. Wang, X. Hu, J. Huang, and P. Pan. 2016. Applicability of simultaneous heat and water model for monitoring late frost injury of winter wheat. *Transactions of the Chinese Society for Agricultural Machinery*, 47(6): 265–274.

[21] Mcmaster, G. S., J. A. Morgan, and W. W. Wilhelm. 1992. Simulating winter wheat spike development and growth. *Agricultural and Forest Meteorology*, 60(3-4): 193–220.

[22] Noi, P., M. Kappas, and J. Degener. 2016. Estimating daily maximum and minimum land air surface temperature using modis land surface temperature data and ground truth data in northern Vietnam. *Remote Sensing*, 08(12): 1002.

[23] Ozelkan, E. C. 2015. Spatial interpolation of climatic variables using land surface temperature and modified inverse distance weighting. *International Journal of Remote Sensing*, 36(4): 1000–1025.

[24] Peng, D. 2009. Basic principle and application of Kalman Filter. *Software Guide*, 08(11): 32–34.

[25] Ren, J., Z. Chen, H. Tang, Q. Zhou, and J. Qin. 2011. Regional crop yield simulation based on crop growth model and remote sensing data. *Transactions of the Chinese Society of Agricultural Engineering*, 27(8): 257–264.

[26] Serrago, R. A., D. J. Miralles, and G. A. Slafer. 2008. Floret fertility in wheat as affected by photoperiod during stem elongation and removal of spikelets at booting. *European Journal of Agronomy*, 28(3): 301–308.

[27] Steinmeyer, F. T., M. Lukac, M. P. Reynolds, and H. E. Jones. 2013. Quantifying the relationship between temperature regulation in the ear and floret development stage in wheat (Triticum aestivum L.) under heat and drought stress. *Functional Plant Biology*, 40(7): 700–707.

[28] Xie, Y., P. Wang, and J. Liu. 2015. Winter wheat yield estimation based on assimilation method combined with 4DVAR and EnKF. *Transactions of the Chinese Society of Agricultural Engineering*, 31(1): 187–195.

[29] Xie, Y., P. Wang, H. Sun, S. Zhang, and L. Li. 2016. Assimilation of leaf area index and surface soil moisture with the CERES-Wheat model for winter wheat yield estimation using a particle filter algorithm. *IEEE Journal of Selected Topics in Applied Earth Observations and Remote Sensing*, 10(4): 1303–1316.

[30] Xu, Y., Z. Qin, and Y. Shen. 2011. Estimation of near surface air temperature from modis data in the Yangtze River Delta. *Transactions of the Chinese Society of Agricultural Engineering*, 27(9): 63–68.

[31] Yan, M., W. Cao, W. Luo, and H. Jiang. 2000. A mechanistic model of phasic and phenological development of wheat I. *Assumption and description of the model. Chinese Journal of Applied Ecology*, 11(3): 355–359.

[32] Yan, M. C., W. X. Cao, C. D. Li, and Z. L. Wang. 2000. Validation and evaluation of a mechanistic model of phasic and phenological development of wheat. *Scientia Agricultura Sinica*, 33(2): 43–50.

[33] Yang, Z. Q. 2007. Corresponding relation between leaf and spikelet primordium differentiation of different development type of wheat cultivars. *Journal of Nuclear Agricultural Sciences*, 21(6): 550–556.

[34] Zun-Fu, L., X. J. Liu, L. Tang, L. L. Liu, W. X. Cao, and Y. Zhu. 2013. Regional prediction and evaluation of wheat phenology based on the WheatGrow and CERES Models. *Scientia Agricultura Sinica*, 46(6): 1136–1148.